Conductivity of carbonized and activated leather waste

Conductivity of carbonized and activated leather waste

Barbora Grycová[a], Kateřina Klemencová[a], Pavel Leštinský[a], Jaroslav Stejskal[b,*], Tomáš Sáha[b], Miroslava Trchová[c], Jan Prokeš[d]

[a]*Institute of Environmental Technology, Centrefor Energy and Environmental Technologies, VSB - Technical University of Ostrava, 708 00 Ostrava, Czech Republic*

[b]*University Institute, Tomas Bata University in Zlin, 760 01 Zlin, Czech Republic*

[c]*University of Chemistry and Technology, Prague, 166 28 Prague 6, Czech Republic*

[d]*Charles University, Faculty of Mathematics and Physics, 180 00 Prague 8, Czech Republic*

[*]Corresponding author. E-mail address: stejskal@utb.cz (J. Stejskal).

ABSTRACT

The conductivity of chromium-tanned pigskin leather waste carbonized in various manner to nitrogen-containing carbons is reported. Four protocols have been tested: (1) The simple carbonization at 800 °C in inert atmosphere, (2) the carbonization at 500 °C followed by the activation with potassium hydroxide at 800 °C, (3) direct activation with the alkali at 800 °C and (4) the similar activation with potassium hydroxide excess. The fibrous collagen morphology was preserved after the carbonization except for some shrinkage. The yield in the simple carbonization, 26.9 wt%, was reduced to 23.9 wt% for the activated products. Elemental analysis indicated reduced content of organic elements after carbonization, and X-ray fluorescence the composition of growing inorganic part. The chromium content in biochar was close to 12 wt% and the X-ray diffraction revealed also the presence of metallic chromium in addition to expected chromium(III) oxide and sulfide. $FTIR$ and Ramanspectroscopies demonstrated the typical pattern of carbonized materials. The specific surface area and pore volume increased after the activation. The resistivity of the powdered carbonized leather was determined in four-point van der Pauw setup. It decreased by more than one order of magnitude as applied pressure increased from 0.1 to 10 MPa. The sample conductivity depended only a little on the way of carbonization and was of the order of tenths to units S cm^{-1} at10 MPa. The precarbonization followed by the activation provided the best result with respect to the yield, nitrogen-content, specific surface area and conductivity of the carbonized material.

Keywords: Activation, carbonization, conductivity, leather waste

1. Introduction

There is a general concern to convert various wastes to products that can be further applied in various directions (**El-Hout et al., 2022; Hemati et al., 2023**). For example, leather waste is generated in the world by vast amounts. The conversion of collagen biopolymer to carbonaceous materials at elevated temperature by carbonization in inert atmosphere has led to variety of useful products, among them the solid biochar being the most often exploited (**Stejskal et al., 2023**). The large-scale uses in the

construction materials are illustrated by the fillers to cement (**Sivaprakash et al., 2017**) or mortar (**Andrade and Mattje 2012**), bitumen binder (**Murugan et al., 2020**) or as a replacement of recycled plastics (**Enfrin and Giustozzi 2022**). In agriculture, the compost additive (**Guo et al., 2020**), a fertilizer (**Kuligowski et al., 2023**) or soil conditioners (**Skrzypczak et al., 2022**) fall to this category. The application as a solid fuel was also proposed (**Kluska et al., 2019; Lee et al., 2019; Li et al., 2023; Sun et al., 2023**). The materials of practical interest are further represented by adsorbents of pollutants, e.g., organic dyes and heavy-metal ions, in water pollution treatment (**Oliveira et al., 2011; Arcibar-Orozco et al., 2019; Gupta et al., 2022; Ke et al., 2022; Pinheiro et al., 2022**) or by the removal of organic vapours (**Rossi et al., 2023**). The materials of this type are likely to be also applicable in hydrogen and carbon dioxide storage (**Ouzzine et al., 2021; Serafin et al., 2023**).

The energy-storage devices currently employ carbons as electrode components. It is not surprising that the carbonized leathers have been successfully tested in supercapacitors (**Konikkara et al. 2016a, 2017; Ma et al., 2019; Liu et al., 2022; El-Hout et al., 2022**), lithium-ion batteries (Ashokkumar et al., 2012; Han et al., 2020) or in electrodes for electrocatalysis (**Alonso-Lemus et al., 2016; Soni et al., 2019; Ke et al., 2022**). For such applications, electrical conductivity is a prerequisite but its quantitative determination has rarely been reported in the literature (**Ashokkumar et al., 2012; Konikkara et al., 2016b**). The reason is obvious: the products of carbonization are obtained as powders that cannot be compressed to pellets used for the routine four-point conductivity determination. Electrical properties thus have to be determined on compressed powder, and the results are dependent on applied pressure. The four-point van der Pauw setup applicable to well-conducing samples has only recently been developed for this purpose (**Stejskal et al., 2022**).

The present study is oriented on the determination of conductivity (or its reciprocal presentation, resistivity), along with other parameters that matter in the design of energy-storage devices, such as specific surface area and elemental composition, with emphasized role of nitrogen and chromium content.

2. Experimental

2.1. Carbonization

Chromium-tanned grey pigskin leather obtained from Bata a. s., Dolní Němčí, Czech Republic) was originally supplied from Garbarnia Nadarzyn (Poland). The leather for pyrolysis experiments was adjusted to the required size with the knife grinder Testchem LMN 100 (Poland) and IKA Tube Mill control (Germany).

Simple carbonization ($sample\ 1$): Preparative carbonizations were carried out at 800 °C in LT tube furnace (LAC, Czech Republic) in inert nitrogen atmosphere with 5.0 quality. The system operated as a batch reactor and, after establishing inert atmosphere, continuous gas flow was not necessary. The selection of 800 °C temperature was based on preliminary series of carbonizations as a compromise between complete conversion to carbons, good level of conductivity, and reasonable yield. The power was switched on and the temperature increased at 5 °C min^{-1} rate to the target temperature and kept there for 3 h. The power was then switched off and the product was left to cool to ambient temperature still under nitrogen atmosphere.

Two-step carbonization/activation ($sample\ 2$): At the beginning, leather was pyrolysed at 500 °C again with heating rate of 5 °C min^{-1} and a residence time of 3 h. The biochar was activated with saturated aqueous solution of potassium hydroxide (Penta, Czech Republic) at 1:1 mass ratio. The mixture was

dried at 105 °C overnight in the Memmert UF55 m dryer (Germany). Activated biochar was pyrolysed in the tube furnace at 800 °C under the same conditions as above.

Direct activation ($sample\ 3$): A mixture of leather with potassium hydroxide solution in the 1:1 mass ratio was prepared. The mixture of both components was dried in a dryer at 105 °C overnight. The resulting solids were pyrolysed at 800 °C as above.

Activation with excess KOH ($sample\ 4$): The same as the preceding procedure but the mass of potassium hydroxide solution was doubled to 1:2 mass ratio.

Washing 1H-4H): This step removed water-soluble part of samples, especially the alkaline residuals after activation, but not necessarily all inorganic components. A part of carbonized leathers 1-4 underwent a treatment with 0.1 M hydrochloric acid. All carbonized leathers were then washed twice with copious amount of hot water (80 °C) and ten times with cold one (20 °C). The solids were left to dry at 105 °C in a dryer overnight, milled, and sieved. For the analysis, the particle size fraction below 0.16 mm was used.

2.2. Characterization

Thermogravimetric analysis was carried out with a TGA 701 apparatus (Leco, USA) in inert nitrogen or in air at heating rate 5 °C min^{-1} in 20-800 °C temperature range.

Scanning electron microscope (Tescan Vega, Czech Republic) displayed the morphology at various magnification. Samples were gold-sputtered prior to microscopy.

Elemental analysis was performed with a CHSN 628 analyzer (Leco, USA) equipped with IR and TC cells. Samples were burned in air at 950 °C for determination of C, H, N elements and in order to determine sulfur content, a temperature of 1350 °C was used. X-ray fluorescence spectrometry (Spectro Xepos, XRF, Germany) was used to quantify inorganic elements in ash.

Phase composition and microstructural properties were determined using X-ray powder diffraction technique. Diffraction patterns were obtained with detector a D/teX Ultra 250. The source of X-ray irradiation was Co tube (CoK_α, $\lambda_1 = 0.178892$ nm, $\lambda_2 = 0.179278$ nm) operated at 40 kV and 40 mA. Incident and diffracted beam optics were equipped with a 5° Soller slits; incident slits were set up to irradiate the sample area 10 × 10 mm^2 constantly (Smartlab, Rigaku Corp., Japan).

$FTIR$ spectra were collected using a Nicolet 6700 spectrometer (Thermo-Nicolet, USA) equipped with a reflective ATR extension GladiATR (PIKE Technologies, USA) with a diamond crystal. Spectra were recorded in the 4000-400 cm^{-1} range at resolution 4 cm^{-1}, 64 scans and Happ-Genzel apodization.

Raman spectra were recorded with a Thermo Scientific DXR Raman microscope operating with a 532 nm laser line. The spot size of the laser was focused by 50 × objective. The scattered light was analysed by a spectrograph with holographic gratings 900 lines mm^{-1} and a pinhole width of 50 μm. The acquisition time was 10 s with 10 repetitions.

Commercial apparatus 3Flex (Micromeritics Ltd., USA) was used for the assessment of surface properties, specific surface area, mesopore surface, and micropore volumes. The measurement was based on nitrogen adsorption at 77 K. Before each experiment, the samples were dried and degassed in 0.06 mbar vacuo at 350 °C for 48 h.

2.3. Electrical properties

The resistivity of the powdered carbonized leathers was determined by using the four-point van der Pauw method employing a lab-made apparatus composed of a cylindrical glass cell with an inner diameter of 10 mm (**Stejskal et al., 2022**). The carbonized powders were placed between a glass support and a glass piston carrying four platinum/rhodium electrodes at the perimeter of its base. The set-up used a current source Keithley 220, a Keithley 2010 multimeter and a Keithley 705 scanner with a Keithley 7052 matrix card. The pressure up to 10 MPa was registered with a L6E3 strain gauge cell (Zemic Europe BV, The Netherlands). The force was applied using an E87H4-B05 stepper motor (Haydon Switch & Instrument Inc., USA).

3. Results and discussion

3.1. Carbonization

The preliminary thermogravimetric analysis provides an insight on the course and yield of the carbonization at analytical scale. When the experiment was carried out in inert nitrogen atmosphere (**Fig. 1**a), the first mass loss took place close to 102 °C and it corresponds to the release of water. The content of humidity in original leather was 12.4 wt%. The carbonization step is centred at relatively low temperature, 343 °C, leaving a residue of 26 wt% at 800 °C. The similar pattern is observed when the analysis is carried out in air (**Fig. 1**b). In addition, the decomposition of the carbonized products takes place in the vicinity of 422 °C and it is completed at 590 °C, leaving about 3 wt% of ash represented by inorganic fraction.

Above analysis provides some guidance for the understanding of the preparative carbonization. Four carbonization at 800 °C have been carried out (**Table 1**), leaving the yields between 23 and 28 wt%. The yields of biochar above 20 wt% can be regarded as still acceptable for the practical preparation of carbonaceous materials.

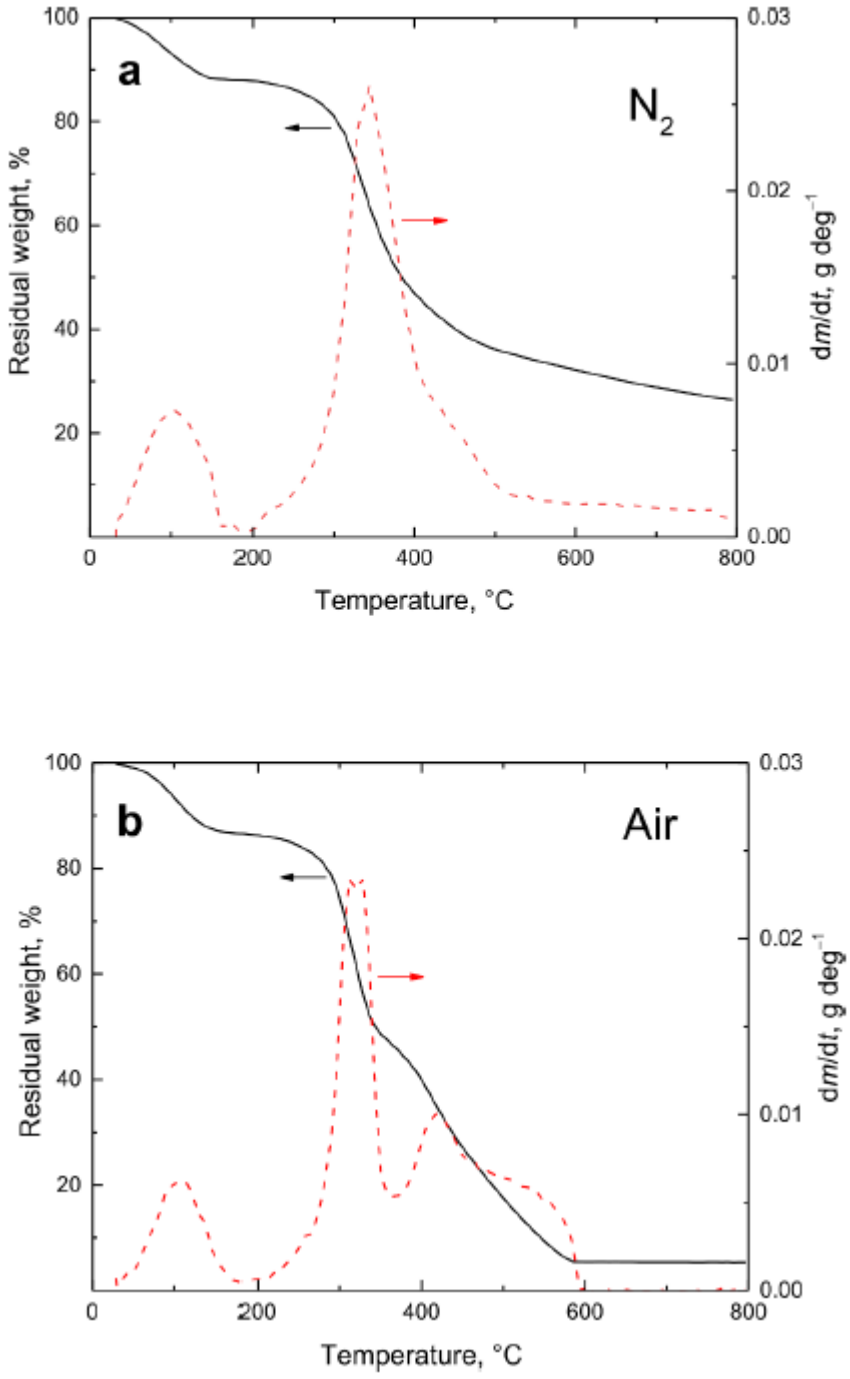

Fig. 1. Thermogravimetric analysis of leather (a) in inert nitrogen and (b) in air.

Table 1 Overview of the carbonization procedures and the yield.

No.	Procedure	Yield, wt%
1	Simple carbonization at 800 °C	26.5
2	Pre-carbonization at 500 °C followed by activation with KOH (1:1) at 800 °C	27.7
3	Direct activation with KOH (1:1) at 800 °C	23.9
4	Activation with excess KOH (1:2) at 800 °C	23.8

3.2. Morphology

The leather is composed of collagen fibres (Fig. 2, top) that fuse after the carbonization (**Fig. 2**, bottom). The connective fibrous structure becomes preserved after carbonization except for some shrinkage. The structural connectivity is the prerequisite for the good electrical conduction of resulting carbons.

3.3. Elemental composition

Elemental analysis reveals the increase in carbon content after carbonization as expected (**Table 2**). The hydrogen atoms are practically eliminated. The simple carbonization (sample 1) leaves a significant fraction of nitrogen atoms that are beneficial for various applications, due to their ability to be hydrogen-bonded to the species in surrounding medium. This is important especially for adsorption phenomena. The content of nitrogen is significantly reduced after activation with potassium hydroxide. At the same time, the content of sulfur increases. The content of ash also increases and the products of extensive activation (e.g., sample 4) are mainly of an inorganic nature. They cannot be regarded as nitrogen-containing carbons any more. Yet, as demonstrated below, they still retain a good level of conductivity.

The participation of inorganic elements in ash (**Table 3**) reveals the dominating presence of chromium, which is separately discussed below. This is followed by the contribution of silicon, aluminium and calcium, as may be expected in natural materials. The activation with potassium hydroxide introduces a significant amount of potassium. The presence of Cl, Ti, P, Mn, Zn, and Ni atoms was detected in amounts below 1 wt%. The sum of all elements corresponds to the amount of ash in the sample. The washing of the samples with hydrochloric acid (samples H) had only a negligible effect on the elemental composition (**Tables 2 and 3**).

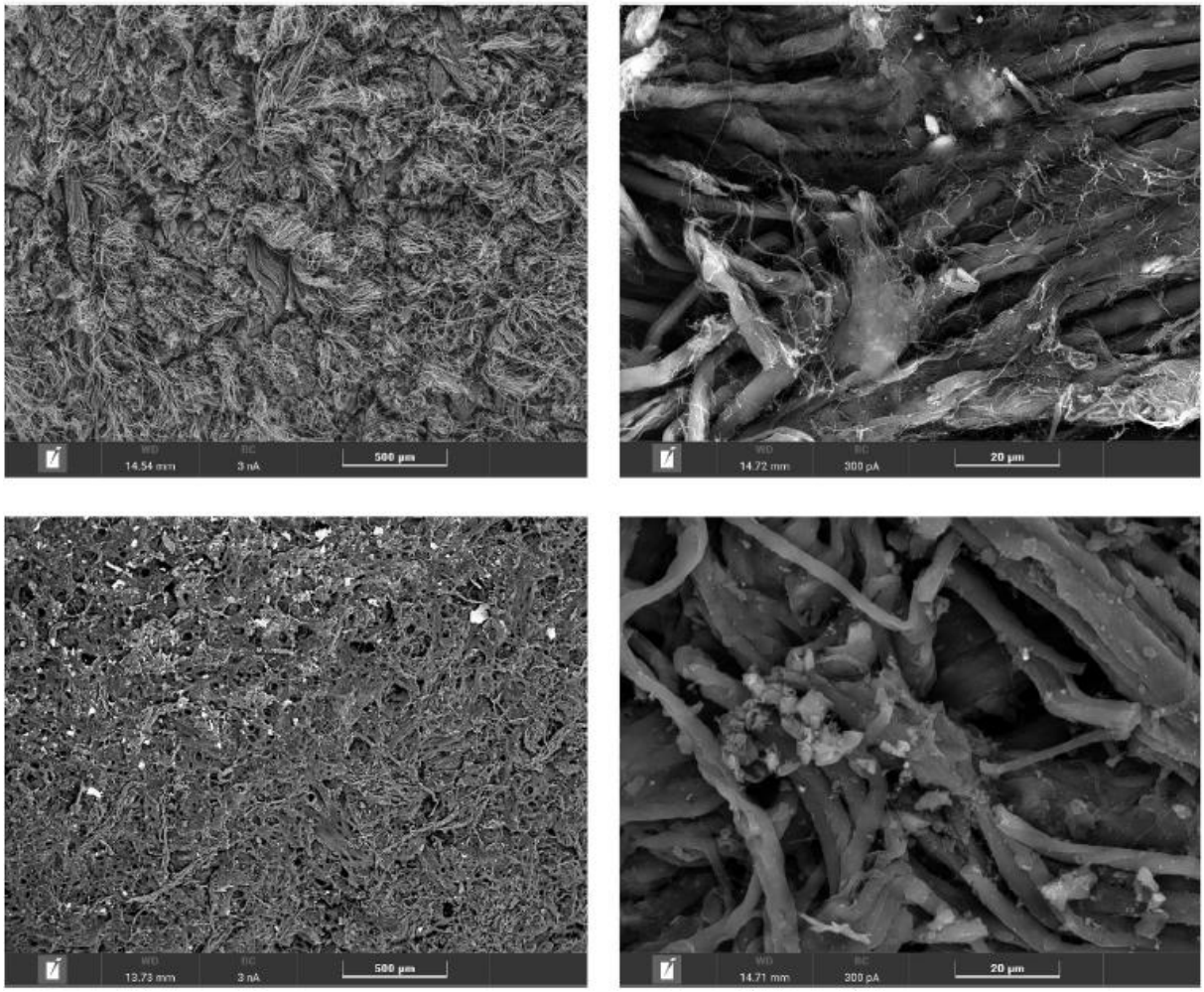

Fig. 2. Scanning electron micrographs of original leather (top) and leather after simple carbonization at 800 °C (bottom) taken at lower (left) and higher magnification (right).

Table 2 The content of organic elements from elemental analysis and the fraction of inorganic part, ash (wt%).

Sample	C	H	N	S	O[a]	Ash
Original	46.67	7.77	14.61	1.72	22.45	6.78
1	70.68	1.06	7.64	0.61	<0.05	20.00
1H	68.48	2.10	7.37	0.65	0.98	20.42
2	66.42	1.79	2.62	0.30	0.95	27.92
2H	66.04	1.26	2.59	0.15	1.39	28.58
3	53.69	0.92	1.59	1.64	0.68	41.48
3H	53.22	0.86	1.80	1.67	0.26	42.19
4	30.93	0.74	0.89	4.01	<0.05	63.41
4H	28.73	0.70	0.86	5.66	<0.05	64.04

[a] *Content of oxygen is calculated to 100%.*

Table 3 The content of inorganic elements in carbonized material (wt%) obtained from the analysis of ash by X-ray fluorescence analysis.

Sample	Cr	Si	Al	Fe	Ca	K
1	12.65	2.87	2.00	0.33	0.40	0.16
1H	12.42	2.74	1.88	0.57	0.42	0.16
2	13.89	2.90	1.95	0.59	1.19	6.56
2H	12.84	3.30	2.30	0.79	1.39	6.99
3	15.54	3.93	2.61	6.35	1.71	6.89
3H	15.65	3.74	2.51	7.10	1.95	6.71
4	19.56	3.71	2.19	(21.87[a])	1.72	5.77
4H	18.67	4.01	2.44	(19.57[a])	1.72	5.98

[a] *Iron content is affected by the corrosion of furnace in aggressive activation medium.*

3.4. Chromium

The presence of chromium is specific for the carbonization products of chrome-tanned leather. Tanning is the process of transforming the skin or hide of various animals into leather. Chromium(III) salts are used for tanning, and the modern plants in use today are still not regarded as eco-friendly. They are used for crosslinking of collagen fibres and become strongly incorporated in leather structure. Despite the non-toxicity of chromium(III), the potential risk of toxic chromium(VI) to the environment and human population in the vicinity of tanneries is suspected, and this applies especially to industrial wastewaters. The presence of chromium(VI) can be completely eliminated in carbonized products (**Fang et al., 2019; Murugan et al., 2020; Zhou et al., 2021**). The typical content of chromium in leather amounts to 4-5 wt% (**Zhou et al., 2021**) and it increases after simple carbonization to 12-13 wt%.

So far unreported chromium metal has been identified with XRD, where significant peaks of metallic chromium (Cr^0) were found at sites 51 and 75°(**Fig. 3**). Chromium has a high metallic conductivity 8 × 10^4 S cm^{-1} at 20 °C. In the composites, the overall conductivity is governed by the volume fraction of conducting component. Due to the high density of chromium, 7.3 g cm^{-3}, the volume fraction of the metal in the composite with carbon can be estimated as 2-3 vol%. Such content of a particulate filler falls below the percolation limit, 17-18 vol%, which sets the onset of composite conduction. For that reason, the presence chromium cannot affect the overall conduction mediated by the carbon matrix.

The peaks of metallic chromium were no longer observed to such an extent in activated samples 2-4 (**Fig. 3**). While the activation will disrupt the surface of carbonaceous material, the reaction of heteroatoms with each other can be achieved and therefore chromium sulfides (Cr_3S_4) or oxides (Cr_2O_3) are formed (**Oliveira et al., 2011; Fang et al., 2018; Arcibar-Orozco et al., 2019; Sun et al., 2021**). The former compound was probably formed by the reaction of chromium with hydrogen sulfide, since raw leather contained about 1.7 wt% sulfur. As a result of the etching of the organic structure, the formed hydrogen sulfide could react with metallic chromium.

In samples 1-3 we can also observe a typical broad graphite peak (8-15°). In the sample 4 it disappeared because the addition of KOH in excess caused complete etching of the organic matter and destruction of its molecular structure. After activation, only about 30 wt% of carbon was present in the sample and the graphite structure was no longer formed during pyrolysis. The peak at 34° in samples 2-4 is assigned to kalsilite ($KAlSiO_4$) which was produced due to chemical activation of samples using potassium hydroxide. The presence of potassium in the activated samples was also confirmed by XRF analysis (**Table 3**).

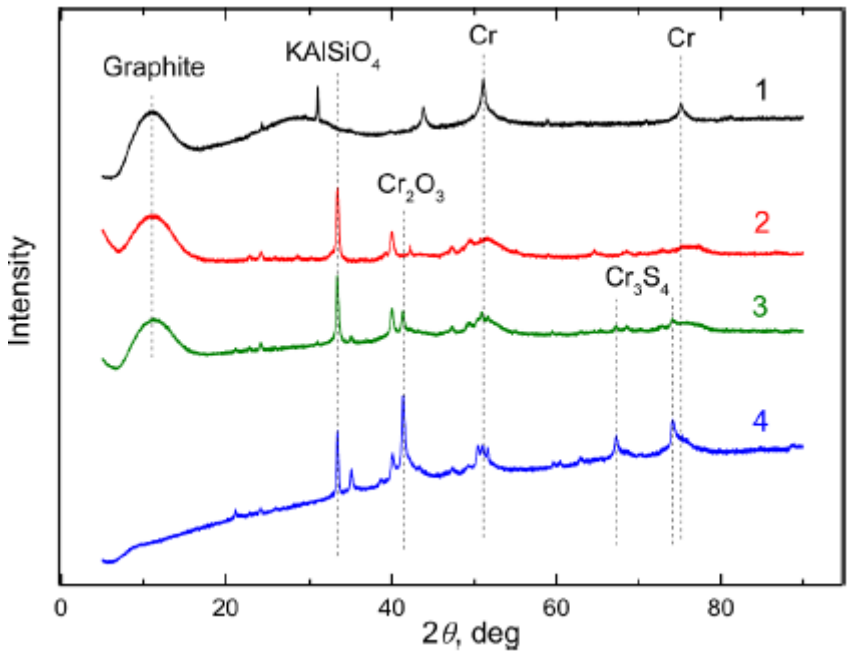

Fig. 3. Wide-angle X-ray diffractograms of carbonized leathers.

3.5. FTIR and Raman spectroscopy

The infrared spectra of the all samples are practically featureless. They correspond to the carbon-like organic part where the Raman active D- and G-bands (see below) are inactive in $FTIR$ spectra. In disordered samples, however, they become IR-active because of symmetry breaking of the carbon network. Two broad maxima situated at 1572 and 1036 cm^{-1} are present in the spectrum of sample 1 prepared by simple carbonization (**Fig. 4**a). The spectrum of sample 2 prepared by two-step process and 3 prepared by direct activation contain in addition to local maximum at 1572 cm^{-1} also two featureless local maxima at 1107 and 968 cm^{-1}, which may be assigned to the residual bands of collagen or impurities introduced by the activation. In the spectrum of sample 4 prepared by the activation with excess KOH these bands are more pronounced and the maxima at 827 and 594 cm^{-1} are observed.

The Raman spectra are typical of carbonaceous materials with two broad bands situated at 1594 cm^{-1} ("G-band" for graphite) and at 1350 cm^{-1} ("D-band" for the disordered form) (**Fig. 4**b). The first originates from the ordered hexagonal rings consisting of conducting sp2-bonded carbon, and the second becomes active only in the presence of structure disorder (**Robertson 2002; Dresselhaus et al., 2008**). The ratio of the intensities of the D- and G-bands is higher for samples 3 and 4 in comparison with samples 1 and 2, which signifies an increase in disorder in former samples.

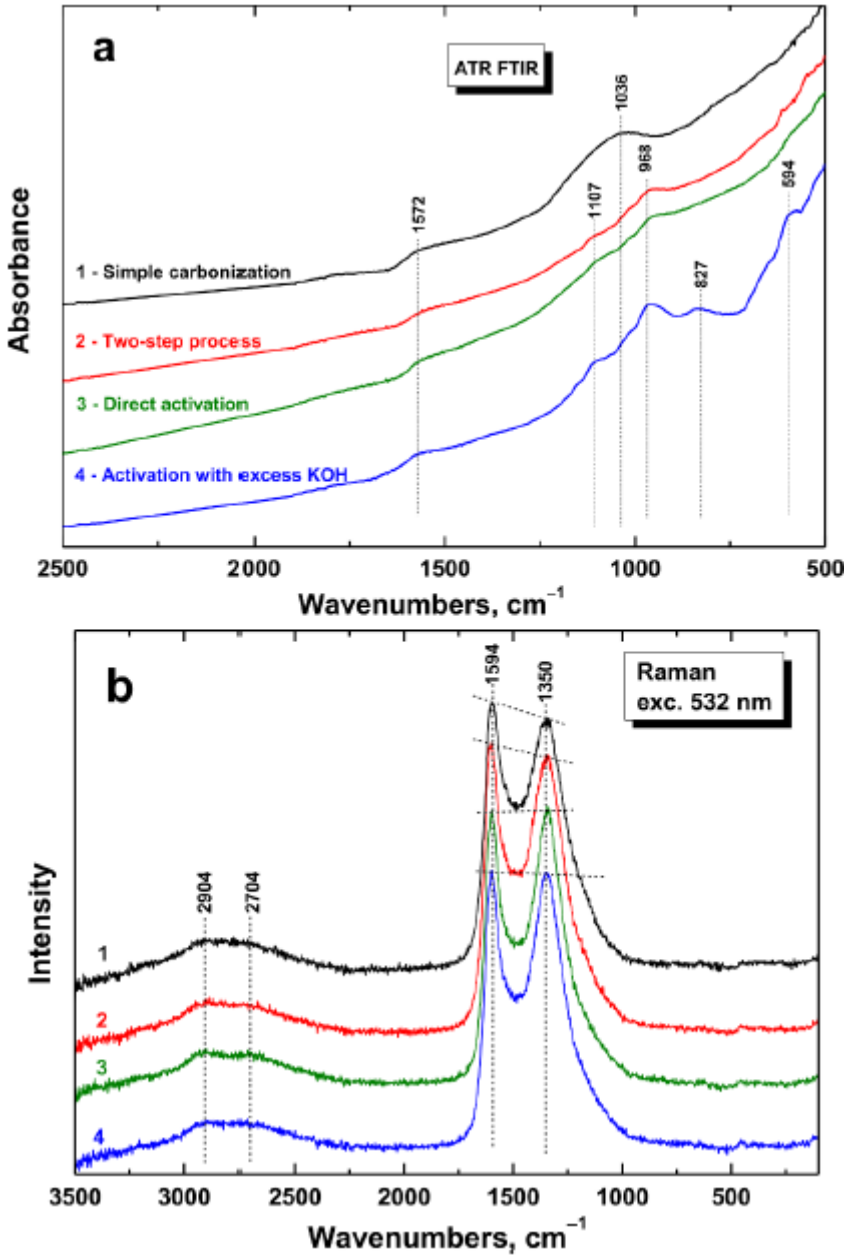

Fig. 4. (a) $FTIR$ and (b) Raman spectra of carbonized leathers (1-4).

3.6. Specific surface area

The specific surface area is important parameter when the carbonaceous materials are planned to be used as adsorbents, electrocatalysts or in supercapacitor electrodes. The simple carbonization yields the samples with low area, here 161 m^2g^{-1} (**Table 4**, **Fig. 5**), often only of the order of units or tens m^2g^{-1} at best (**Oliveira et al. 2008, 2011; Colmenares et al., 2014**). The activation, e.g., the carbonization in the presence of potassium hydroxide, increases this parameter to hundreds or even a few thousands m^2g^{-1} (**Ma et al., 2019; Han et al., 2020; Liu et al., 2020; Cabrera-Codony et al., 2021**). The porosity increases accordingly (**Table 4**). The extensive activation, however, is not favourable. Except for the simple carbonization, the washing had negligible effect on the properties. For above applications mentioned above, the presence of nitrogen atoms is important due to their ability to participate in

hydrogen bonding in aqueous media. Here, the activation strongly reduces or even eliminates the nitrogen content in the chars (**Table 2**). From this point of view, a two-step process based on the precarbonization followed by activation seems to be the best compromise.

3.7. Resistivity

Electrical properties of carbonized leather have been reported so far rarely (**Ashokkumar et al., 2012; Konikkara et al., 2016b; Stejskal et al., 2023**) due to technical difficulties. The final products of carbonization are obtained as powders that cannot be compressed to free-standing pellets used for the routine conductivity determination. For that reason, the powder has to be characterized in compressed state and the conductivity (or the reciprocal quantity, a resistivity) depends on the applied pressure (**Fig. 6**). So far, the two-probe measurement has been reported in the literature (**Ashokkumar et al., 2012; Konikkara et al., 2016b**), which suggested a good level of conductivity. For such conducting samples, however, the four-point measurement in van der Pauw setup is more appropriate and was applied in the present study.

The resistivity of the carbonized materials decreased with applied pressure (**Fig. 6**). The absolute value of the slope of this dependence reflects the compressibility of the samples, i.e. how easily is the volume reduced in the response to applied pressure. The present samples yield to the pressure as may be expected for organic rather than inorganic materials. At the reference pressure, here 10 MPa, the conductivity of samples is of the order of tenths and units S cm^{-1} (**Table 4**), i.e. at the level found in conducting polymers, such as polypyrrole (**Stejskal et al., 2023**). This is an important result as in some applications of conducting polymers, the carbonized leather may be an economic replacement. The results also indicate that the way of carbonization had no significant effect on the conductivity of products; the differences within one order of magnitude can be regarded as small (**Table 4**).

Table 4 Specific surface area (BET) and the area of mesopores, S, micropore and total pore volume, V, median pore width, d, and conductivity, a, determined under 1 and 10 MPa pressure before and after washing (H).

Sample	S, m^2g^{-1}		V, cm^3g^{-1}		d, nm	σ, S cm^{-1}	
	BET	Mesopores (2–50 nm)	Micropores (< 2 nm)	total	pore width	1 MPa	10 MPa
1	161	4.6	0.079	0.087	0.52	0.050	0.22
1H	298	64.4	0.116	0.178	0.51	0.047	0.23
2	1170	96.7	0.504	0.603	0.48	0.31	1.39
2H	1180	107	0.507	0.616	0.49	0.37	1.41
3	928	190	0.342	0.519	0.51	0.51	1.69
3H	888	179	0.329	0.495	0.51	0.28	1.01
4	511	177	0.156	0.351	0.54	0.19	0.71
4H	519	198	0.158	0.374	0.54	0.20	0.75

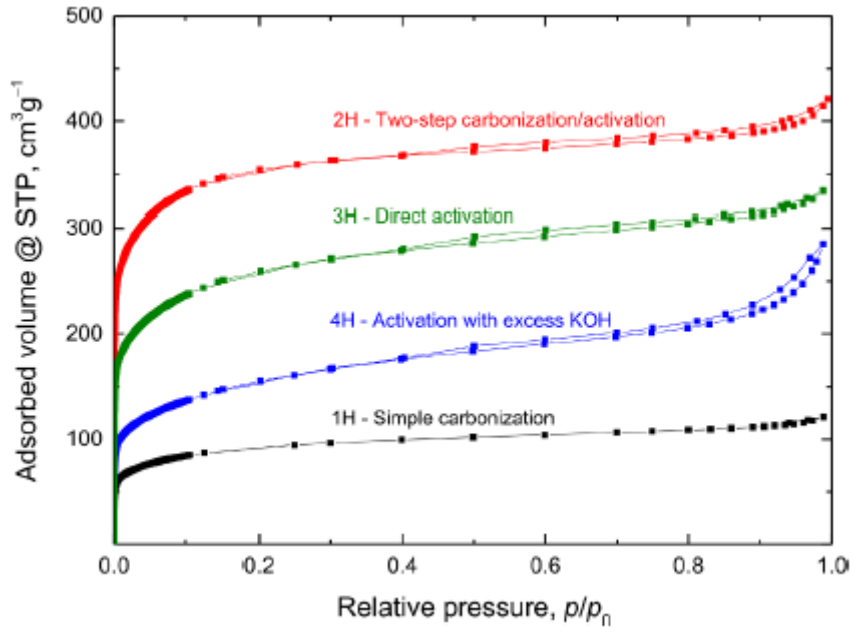

Fig. 5. The adsorption/desorption isotherms of carbonized leathers.

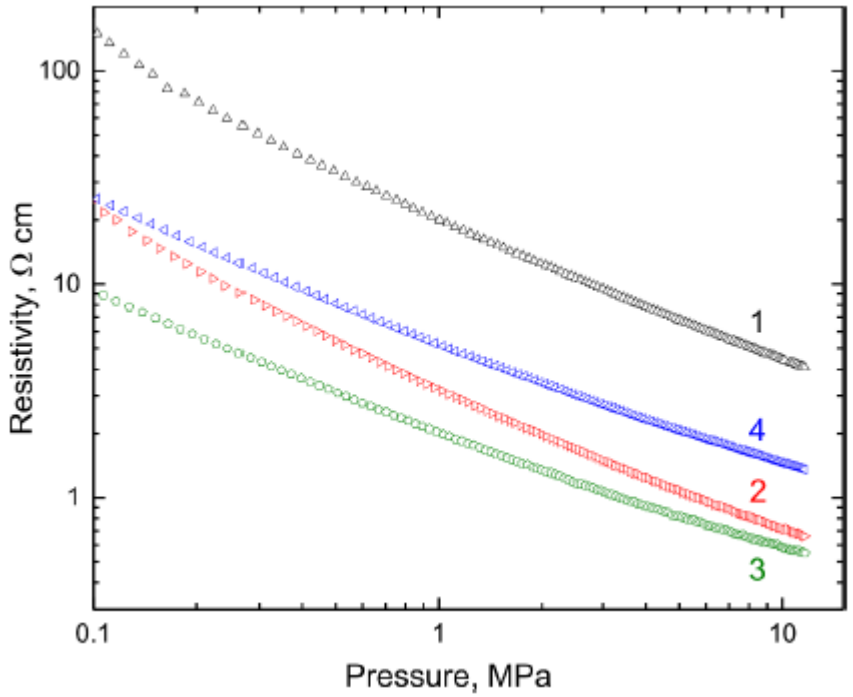

Fig. 6. The dependence of the resistivity of carbonized leather on applied pressure. 1 - simple carbonization, 2 - two-step carbonization/activation, 3 - direct activation, 4 - activation with excess KOH.

4. Conclusions

The effect of carbonization protocol on the conductivity of products was the primary goal to test. Four types of leather carbonization and activation have been carried out. All products have been obtained in comparable yield 23-28 wt% and they had similar conductivity of the order of tenths to units, 10^{-1}-

10° S cm^{-1}, determined on powders compressed at 10 MPa. Such conductivity is comparable with that of conducting polymers, such as polypyrrole (**Stejskal et al., 2023**). The extensive washing with dilute acid and water meant to remove soluble inorganics and activation residues, had no significant effect on electrical properties. The samples differed, however, in the specific surface area. The simple carbonization at 800 °C yielded the product with relatively low area, 161 m^2g^{-1}, which increased to 1180 m^2g^{-1} in two-step precarbonization/activation procedure. The content of ash increased from 20 wt% for simple carbonization to 64 wt% for the activation with excess of potassium hydroxide, indicating the gradual loss of organic carbon from 71 wt% to 28 wt% and nitrogen from 8 wt% to 1 wt%. While the product of simple carbonization can be regarded as a nitrogen-containing carbon, the extensive activation may lead to mainly inorganic material without any relation to the original leather structure. Chromium was found in all samples, from 13 wt% in metallic state after simple carbonization to 20 wt% after activation in chromium(III) oxide or sulfide. The presence of metallic chromium is regarded as positive for potential electrocatalytic applications. The two-step process, when the precarbonization 500 °C was followed by the activation at 800 °C, is the best carbonized material with optimized yield, nitrogen and chromium contents, specific surface area, and conductivity.

References

Alonso-Lemus, I.L., Rodriguez-Varela, F.J., Figueroa-Torres, M.Z., Sanchez-Castro, M.E., Hernandez-Ramírez, A., Lardizabal-Gutierrez, D., Quintana-Owen, P., 2016. Novel self-nitrogen-doped porous carbon from waste leather as highly active metal-free electrocatalyst for the ORR. Int. J. Hydrogen Energy 41, 23409-23416. **https://doi.org/10.1016/j.ijhydene.2016.09.033**.

Andrade, J.J.D., Mattje, V., 2012. Incorporation of chromium-tanned leather residue in mortars. Proc. Inst. Civil Eng., Construct. Mater. 165, 73-86. **https://doi.org/10.1680/coma.10.00026**.

Arcibar-Orozco, J.A., Barajas-Elias, B.S., Caballero-Briones, F., Nielsen, L., Rangel-Mendez, J.R., 2019. Hybrid carbon nanochromium composites prepared from chrome-tanned leather shavings for dye adsorption. Water Air Soil Pollut. 230, 142. **https://doi.org/10.1007/s11270-019-4194-x**.

Ashokkumar, M., Narayanan, N.T., Reddy, A.L.M., Gupta, B.K., Chandrasekaran, B., Talapatra, S., Ajayan, P.M., Thanikaivelan, P., 2012. Transforming collagen wastes into doped nanocarbons for sustainable energy applications. Green Chem. 14, 1689-1695. **https://doi.org/10.1039/c2gc35262a**.

Cabrera-Codony, A., Ruiz, B., Gil, R.R., Popartan, L.A., Santos-Clotas, E., Martin, M.J., Fuente, E., 2021. From biocollagenic waste to efficient biogas purification: applying circular economy in the leather industry. Environ. Technol. Innov. 21, 101229. **https://doi.org/10.1016/j.eti.2020.101229**.

Colmenares, J.C., Lisowski, P., Bermudez, J.M., Cot, J., Luque, R., 2014. Unprecedented photocatalytic activity of carbonized leatherskin residues containingchromium oxide phases. Appl. Catal. B Environ. 150, 432-437. **https://doi.org/10.1016/j.apcatb.2013.12.038**.

Dresselhaus, M.S., Dresselhaus, G., Hofmann, M., 2008. Raman spectroscopy as a probe of graphene and carbon nanotubes. Phil. Trans. Roy. Soc. A 366, 231-236. **https://doi.org/10.1098/rsta.2007.2155**.

El-Hout, S.I., Attia, S.Y., Mohamed, S.G., Abdelbasir, S.M., 2022. From waste to value-added products: evaluation of activated carbon generated from leather waste for supercapacitor applications. J. Environ. Manag. 304, 114222. **https://doi.org/10.1016/j.jenvman.2021.114222**.

Enfrin, M., Giustozzi, F., 2022. Recent advances in the construction of sustainable asphalt roads with recycled plastic. Polym. Int. 71, 1316-1383. **https://doi.org/ 10.1002/pi.6405**.

Fang, C.Q., Jiang, X.G., Lv, G.J., Yan, J.H., Deng, X.B., 2018. Nitrogen-containing gaseous products of chrome-tanned leather shavings during pyrolysis and combustion. Waste Manag. 78, 553-558. **https://doi.org/10.1016/j.wasman.2018.06.028**.

Fang, C.Q., Jiang, X.G., Lv, G.J., Yan, J.H., Lin, X.L., Song, H.B., Cao, J.J., 2019. Pyrolysis characteristics and Cr speciation of chrome-tanned leather shavings: influence of pyrolysis temperature. Energy Sources 41, 881-891. **https://doi.org/10.1080/15567036.2018.1520366**.

Guo, X.X., Liu, H.T., Zhang, J., 2020. The role of biochar in organic waste composting and soil improvement: a review. Waste Manag. 102, 844-899. **https://doi.org/ 10.1016/j.wasman.2019.12.003**.

Gupta, R., Pandit, C., Pandit, S., Gupta, P.K., Lahiri, D., Agarwal, D., Pandey, S., 2022. Potential and future prospects ofbiochar-based materials and their applications in removal of organic contaminants from industrial wastewater. J. Mater. Cycles Waste Manag. 24, 852-876. **https://doi.org/10.1007/s10163-022-01391-z**.

Han, W.Y., Wang, H.L., Xia, K.D., Chen, S.S., Yan, P.X., Deng, T.S., Zhu, W.B., 2020. Superior nitrogen-doped activated carbon materials for water cleaning and energy storing prepared from renewable leather wastes. Environ. Int. 142, 105846. **https://doi.org/10.1016/j.envint.2020.105846**.

Hemati, S., Udayakumar, S., Wesley, C., Biswal, S., Nur-A-Tomal, M.S., Sarmadi, N., Pahlevani, F., Sahajwalla, V., 2023. Thermal transformation of secondary resources of carbon-rich wastes into valuable industrial applications. J. Compos. Sci. 7, 8. **https://doi.org/10.3390/jcs7010008**.

Ke, L., Zhao, K., Yan, X.Y., Cao, X.J., Wu, X.Y., Zhang, C., Luo, T.T., Ding, T., Yan, N., 2022. Facile mineralization and valorization of Cr-containing leather shavings for electrocatalytic H2O2 generation and organic pollutant removal. Chem. Eng. J. 437, 135036. **https://doi.org/10.1016/j.cej.2022.135036**.

Kluska, J., Ochnio, M., Kardas, D., Heda, L., 2019. The influence of temperature on the physicochemical properties of products of pyrolysis of leather-tannery waste. Waste Manag. 88, 248-256. **https://doi.org/10.1016/j.wasman.2019.03.046**.

Konikkara, N., Kennedy, L.J., Vijaya, J.J., 2016a. Preparation and characterization of hierarchical porous carbons derived from solid leather waste for supercapacitor applications. J. Hazard Mater. 318, 173-185. **https://doi.org/10.1016/j.jhazmat.2016.06.037**.

Konikkara, N., Kennedy, L.J., Aruldoss, U., Vijaya, J.J., 2016b. Electrical conductivity studies of nanoporous carbon derived from leather waste: effect of pressure, temperature and porosity. J. Nanosci. Nanotechnol. 16, 8829-8838. **https://doi.org/10.1166/jnn.2016.11652**.

Konikkara, N., Punithavelan, N., Kennedy, L.J., Vijaya, J.J., 2017. A new approach to solid waste management: fabrication of supercapacitor electrodes from solid leather wastes using aqueous KOH electrolyte. Clean Technol. Environ. Policy 19, 1087-1098. **https://doi.org/10.1007/s10098-016-1301-1**.

Kuligowski, K., Cenian, A., Konkol, I., Swierczek, L., Chojnacka, K., Izydorczyk, G., Skrzypczak, D., Bandrow, P., 2023. Application of leather waste fractions and their biochars as organic fertilisers for ryegrass growth: agri-environmental aspects and plants response modelling. Energies 16, 3883. **https://doi.org/10.3390/ en16093883**.

Li, M.R., Li, Y.C., Liu, J., Cao, S., 2023. Combustion characteristics and kinetic analysis of finished leather waste using TG-DSC and transformation behavior of Cr during its combustion. Biomass Conv. Biorefinery, early access. **https://doi.org/10.1007/s13399-023-03974-8**.

Lee, J., Hong, J., Jang, D., Park, K.Y., 2019. Hydrothermal carbonization of waste from leather processing and feasibility of produced hydrochar as an alternative solid fuel. J. Environ. Manag. 247, 115-120. **https://doi.org/10.1016/j.jenvman.2019.06.067**.

Liu, Y.H., Zhang, X.F., Gu, X., Wu, N.X., Zhang, R.N., Shen, Y., Zheng, B., Wu, J.S., Zhang, W.N., Li, S., 2020. One-step turning leather wastes into heteroatom doped carbon aerogel for performance enhanced capacitive deionization. Microporous Mesoporous Mater. 303, 110303. **https://doi.org/10.1016/ j.micromeso.2020.110303**.

Liu, P.Y., Xing, Z.H., Wang, X., Diao, S., Duan, B.R., Yang, C., Shi, L., 2022. Nanoarchitectonics of nitrogen-doped porous carbon derived from leather wastes for solid-statesupercapacitor. J. Mater. Sci. Mater. Electron. 33, 4887-4901. **https://doi.org/10.1007/s10854-021-07678-5**.

Ma, F., Ding, S.L., Ren, H.J., Peng, P.L., 2019. Preparation of chrome-tanned leather shaving-based hierarchical porous carbon and its capacitance properties. RSC Adv. 9, 18333-18343. **https://doi.org/10.1039/c9ra03139a**.

Murugan, K.P., Balaji, M., Kar, S.S., Swarnalatha, S., Sekaran, G., 2020. Nano fibrous carbon produced from chromium bearing tannery solid waste as the bitumen modifier. J. Environ. Manag. 270, 110882. **https://doi.org/10.1016/j.jenvman.2020.110882**.

Oliveira, L.C.A., Guerreiro, M.C., Gonsalves, M., Oliveira, D.Q.L., Costa, L.C.M., 2008. Preparation of activated carbon from leather waste: a new material containing small particle of chromium oxide. Mater. Lett. 62, 3710-3712. **https://doi.org/10.1016/j.matlet.2008.04.064**.

Oliveira, L.C.A., Coura, C.V., Guimaraes, L.R., Goncalves, M., 2011. Removal of organic dyes using Cr-containing activated carbon prepared from leather waste. J. Hazard. Mater. 192, 1094-1099. **https://doi.org/10.1016/j.jhazmat.2011.06.014**.

Ouzzine, M., Serafin, J., Srenscek-Nazzal, J., 2021. Single step preparation of activated biocarbons derived from pomegranate peels and their CO2 adsorption performance. J. Anal. Appl. Pyrolysis 160, 105538. **https://doi.org/10.1016/j.jaap.2021.105338**.

Pinheiro, N.S.C., Perez-Lopez, O.W., Gutterres, M., 2022. Solid leather wastes as adsorbents for cationic and anionic dye removal. Environ. Technol. 43, 1285-1293. **https://doi.org/10.1080/09593330.2020.1825531**.

Robertson, J., 2002. Diamond-like amorphous carbon. Mater. Sci. Eng. R 37, 129-281. **https://doi.org/10.1016/S0927-796X(02)00005-0**.

Rossi, D., Caúello, M., Antognoli, M., Brunazzi, E., Seggiani, M., 2023. Pyrolyzed tannery sludge as adsorbent of volatile organic compounds from tannery air emissions. Chem. Eng. J. 454, 140320. **https://doi.org/10.1016/j.cej.2022140320**.

Serafin, J., Dziejarski, B., Cruz, Jr, O.F., Srenscek-Nazzal, J., 2023. Design of highly microporous activated carbons based on walnut shell biomass for H2 and CO2 storage. Carbon 201, 633-647. **https://doi.org/10.1016/j.carbon.2022.09.013**.

Sivaprakash, K., Maharaja, P., Pavithra, S., Boopathy, R., Sekaran, G., 2017. Preparation of light weight constructional materials from chrome containing buffing dust solid waste generated in leather industry. J. Mater. Cycles Waste Manag. 19,. **https://doi.org/10.1007/s10163-016-0494-z. 828-838**.

Skrzypczak, D., Szopa, D., Mikula, K., Izydorczyk, G., Basladynska, S., Hoppe, V., Pstrowska, K., Wzorek, Z., Kominko, H., Kulazynski, M., Moustakas, K., Chojnacka, K., Witek-Krowiak, A., 2022. Tannery waste-derived biochar as a carrier of micronutrients essential to plants. Chemosphere 294, 133720. **https://doi.org/10.1016/ j.chemosphere.2022.133720**.

Soni, R., Bhange, S.N., Kurungot, S., 2019. A 3-D nanoribbon-like Pt-free oxygen reduction reaction electrocatalyst derived from waste leather for anion exchange membrane fuel cells and zinc-air batteries. Nanoscale 11, 7893-7902. **https://doi.org/10.1039/c9nr00977a**.

Stejskal, J., Vilčáková, J., Jurča, M., Fei, H.J., Trchová, M., Kolská, Z., Prokeš, J., Křivka, I., 2022. Polypyrrole-coated melamine sponge as a precursor for conducting macroporous nitrogen nitrogen-containing carbons. Coatings 12, 324. **https://doi.org/10.3390/coatings12030324**.

Stejskal, J., Ngwabebhoh, F.A., Sáha, P., Prokeš, J., 2023. Carbonized leather waste: a review and conductivity outlook. Polymers 15, 1028. **https://doi.org/10.3390/ polym15041028**.

Sun, X.G., Peng, Q.F., Wang, Z.X., Li, C.M., Huang, Y.Q., 2021. N-doped porous carbon derived from Cr-tanned leather shaving wastes for synergetic adsorption of Cr (VI) from aqueous solution. Mater. Lett. 284, 128815. **https://doi.org/10.1016/j.matlet.2020.128815**.

Sun, G., Tang, W., Gu, Q.B., Li, L., Duan, Y.Q., Chen, Y.Q., Lu, X.Y., Sun, Z.K., Qian, X.D., Duan, L.B., 2023. Reaction mechanisms and N-containing compound formation during shoe manufacturing waste pyrolysis. Fuel Process. Technol. 244, 107699. **https://doi.Org/10.1016/j.fuproc.2023.107699**.

Zhou, Y.C., Chen, Z.Z., Gong, H.J., Yang, Z.Y., 2021. Chromium speciation in tannery sludge residues after different thermal decomposition processes. J. Clean. Prod. 314, 128071. **https://doi.org/10.1016/j.jclepro.2021.128071**.